

# 纳米孪晶强化304奥氏体不锈钢的应变控制 疲劳行为



潘庆松 崔方 陶乃镛 卢磊

(中国科学院金属研究所 沈阳材料科学国家研究中心 沈阳 110016)

**摘要** 利用动态塑性变形工艺制备块体纳米孪晶强化304奥氏体不锈钢样品并研究其低周疲劳行为。应变控制疲劳测试发现,包含30% (体积分数)纳米孪晶结构的304奥氏体不锈钢具有优异的低周疲劳寿命和高循环应力水平,同时循环软化程度随应变幅增加而减弱,与传统纳米结构金属材料“应变幅愈高,软化程度愈明显”的趋势截然不同。优异的低周疲劳性能主要得益于高强度纳米孪晶晶粒优异的结构稳定性以及其与相邻再结晶晶粒协同塑性变形,有效抑制应变局域化和疲劳裂纹萌生。

**关键词** 纳米孪晶,奥氏体不锈钢,循环响应,疲劳寿命,应变非局域化

中图分类号 TG146

文章编号 0412-1961(2022)01-0045-09

## Strain-Controlled Fatigue Behavior of Nanotwin-Strengthened 304 Austenitic Stainless Steel

PAN Qingsong, CUI Fang, TAO Nairong, LU Lei

*Shenyang National Laboratory for Materials Science, Institute of Metal Research, Chinese Academy of Sciences, Shenyang 110016, China*

Correspondent: LU Lei, professor, Tel: (024)23971939, E-mail: llu@imr.ac.cn

Supported by National Natural Science Foundation of China (Nos.51931010, 92163202, 52122104, and 52071321), Key Research Program of Frontier Science and International Partnership Program, Chinese Academy of Sciences (No.GJHZ2029), Liaoning Revitalization Talents Program (No.XLYC1802026), and Youth Innovation Promotion Association, Chinese Academy of Sciences (No.2019196)

Manuscript received 2021-08-17, in revised form 2021-09-04

**ABSTRACT** Engineering nano-scale twin boundaries has been recognized as a novel strategy to achieve a superior combination of tensile strength, ductility, and fatigue limit in metallic materials. However, to date, the strain-controlled fatigue behavior of nanotwin (NT)-strengthened metals is still rarely explored, most possibly owing to the difficulty in preparing bulk fatigue samples. In this work, a bulk heterogeneously structured 304 stainless steel (304 SS) containing 30% volume fraction of NT bundles embedded in the micrometer-sized grain matrix was prepared and studied under constant plastic strain amplitude-controlled fatigue tests. A considerable fatigue life and much higher cyclic flow stress level, while maintaining a weaker degree of cyclic softening at larger strain amplitude, was achieved in NT-strengthened 304 SS, compared with its coarse-grained counterpart in the same strain-controlled fatigue tests. This is fundamentally distinct from the more obvious softening behavior of conventional nanostructured metals induced by strain localization at larger strain amplitude. Such exceptional low-cycle fatigue

资助项目 国家自然科学基金项目 Nos.51931010、92163202、52122104 和 52071321, 中国科学院前沿科学重点研究计划项目 No.GJ-HZ2029, 辽宁省兴辽英才计划项目 No.XLYC1802026, 及中国科学院青年创新促进会项目 No.2019196

收稿日期 2021-08-17 定稿日期 2021-09-04

作者简介 潘庆松,男,1985年生,副研究员

通讯作者 卢磊, llu@imr.ac.cn, 主要从事块体纳米结构金属材料研究

DOI 10.11900/0412.1961.2021.00342

properties were attributed to the presence of a high-strength NT structure associated with novel mechanical stability and its co-deformation with surrounding grains, effectively suppressing strain localization and fatigue crack initiation.

**KEY WORDS** nanotwin, austenitic stainless steel, cyclic response, fatigue life, strain delocalization

工程构件服役条件复杂,不仅涉及高周疲劳,其孔或缺口等局部位置由于应力集中,往往处于低周疲劳的环境<sup>[1]</sup>。同时具有优异高周与低周疲劳性能是保障工程构件长期安全服役的关键<sup>[1,2]</sup>。研究<sup>[1,2]</sup>表明,金属材料的应力控制高周疲劳性能(如疲劳极限)往往取决于其强度:强度增加,疲劳裂纹萌生阻力增加,疲劳极限提高;而应变控制低周疲劳性能(如疲劳寿命)主要与材料塑性相关:塑性越好,可累积更大塑性变形,并且可降低疲劳裂纹扩展速率,有利于低周疲劳寿命提高。迄今为止,传统强化策略如第二相强化<sup>[3-7]</sup>、应变或纳米结构强化<sup>[8-11]</sup>等可显著提高工程金属材料的强度和高周疲劳极限,但也明显降低塑性和低周疲劳性能。例如,传统高强度超细晶或纳米晶材料具有优异的高周疲劳极限,但应变控制疲劳时往往发生严重循环软化,疲劳寿命相比于粗晶材料明显降低<sup>[8,11-13]</sup>。其根本原因为高能量状态大角晶界易引起结构非稳定化、严重应变局域化和不可逆损伤(如异常晶粒长大和剪切带等)<sup>[2,14,15]</sup>。因此,高周和低周疲劳性能之间不可兼顾的倒置关系已成为制约高强度纳米结构材料走向工业应用的关键瓶颈问题。

近年来,引入纳米尺度孪晶界面被公认是优化材料综合力学性能的一种有效策略<sup>[16-19]</sup>。与传统纳米结构金属不同,这种具有高密度、低能态共格界面的纳米孪晶金属不仅拥有高强度,亦保持良好塑性和机械稳定性等优异力学行为<sup>[20-23]</sup>,尤其在交变循环载荷条件下还彰显出高疲劳极限、长疲劳寿命以及与疲劳历史无关的循环稳定性等优异疲劳特征<sup>[24-26]</sup>,这主要归因于其稳定的共格界面特征以及独特的位错与孪晶界面交互作用<sup>[27-29]</sup>。近期研究<sup>[4,30-35]</sup>表明,引入一定体积分数的纳米孪晶结构亦可显著提高材料的力学和高周疲劳性能。例如,动态塑性变形(DPD)结合后续退火工艺制备的变形纳米孪晶/再结晶混合结构304奥氏体不锈钢的高周疲劳极限和疲劳比分别高达330 MPa和0.36,相对传统粗晶结构(170 MPa、0.22)明显提高<sup>[34]</sup>。在疲劳过程中,纳米孪晶晶粒与周围再结晶晶粒可通过位错运动、马氏体相变等多种变形方式协调疲劳变形,有效抑制了循环应变局域化和疲劳裂纹萌生<sup>[34]</sup>。

为了进一步研究纳米孪晶混合结构的循环应力

响应和疲劳机制,本工作利用DPD及后续退火处理制备了块体纳米孪晶强化304不锈钢(304 SS)样品,通过塑性应变控制低周疲劳实验并结合微观结构表征,研究了纳米孪晶强化304 SS的应变控制低周疲劳性能及其机制。

## 1 实验方法

本工作所用304 SS化学成分(质量分数,%)为Fe-18.29Cr-8.10Ni-0.061C-0.44Si-1.30Mn-0.006S-0.078P。首先在1473 K退火2 h,得到平均晶粒尺寸为180  $\mu\text{m}$ 的退火态粗晶304奥氏体不锈钢。利用DPD技术在大冲击能量(约2.5 kJ)和473 K条件下对直径20 mm、高度14 mm的圆柱体粗晶304样品进行多道次的变形处理,应变速率为 $10^2\sim 10^3\text{ s}^{-1}$ ,累积应变约为1.3,成功制备了直径约为43 mm、高度为3.7 mm的块体纳米孪晶/位错结构样品,其经1003 K退火1 h后得到纳米孪晶/再结晶样品。此外,为了对比,对原始304 SS在723 K退火1 h,获得由等轴状晶粒组成的粗晶304 SS样品,平均晶粒尺寸为46  $\mu\text{m}$ 。宏观疲劳试样标距尺寸为12.0 mm  $\times$  2.0 mm  $\times$  3.5 mm。为了观察表面疲劳特征,疲劳测试前对样品进行了室温电解抛光,抛光电压为16 V,抛光时间为30~60 s,抛光液成分(体积分数)为8% $\text{HClO}_4$ 和92% $\text{CH}_2\text{CH}_2\text{OH}$ 混合溶液。利用Qness Q10A + Vickers硬度计测量纳米孪晶强化304 SS的硬度,测试载荷为20 g,保载时间为10 s。测量100个不同位置纳米孪晶结构的硬度以获得其平均硬度。

使用Instron 8874试验机进行塑性应变控制对称拉-压疲劳实验,应变速率为 $2 \times 10^{-3}\text{ s}^{-1}$ ,控制波形为三角波。在疲劳过程中,采用标距长度为10 mm的Instron 2620-603夹持式引伸计测量并控制疲劳应变幅。疲劳实验停止条件为应力幅下降为最大应力幅的50%或疲劳寿命达到 $10^5\text{ cyc}$ 。

利用LEXT OLS4000激光共聚焦显微镜(CLSM)表征不同应变幅疲劳后纳米孪晶强化304 SS样品表面滑移带三维形貌。其中,定义滑移带相邻波峰与波谷的高度差为起伏高度( $h$ )。基于大量数据统计(至少200个)获得纳米孪晶和再结晶结构表面滑移带平均起伏高度。采用Nano-SEM-Nova 460场发射扫描电镜(SEM)和Tecnai F20透射电子显



显微镜(TEM)分别表征制备态和疲劳后纳米孪晶强化304 SS样品的微观结构。通过统计超过100张SEM照片中纳米孪晶区域所占总面积的比例记为纳米孪晶的平均体积分数。采用化学双喷电解减薄工艺制备TEM样品,双喷电压为25~30 V,电流为35~45 mA,温度为-20~-15°C,双喷液成分(体积分数)为8% $\text{HClO}_4$ 和92% $\text{CH}_3\text{CH}_2\text{OH}$ 混合溶液。

## 2 实验结果

DPD 304 SS的微观结构为纳米尺度变形孪晶结构呈“岛状”分布于位错结构基体<sup>[34]</sup>。图1为纳米孪晶强化304 SS的微观结构:DPD样品在退火时位错结构优先发生再结晶(图1a)。大部分再结晶晶粒呈等轴状,晶界平直明锐,晶内干净,无位错残留(图1b),平均晶粒尺寸为3.5  $\mu\text{m}$ 。大部分纳米孪晶结构在退火过程中十分稳定(图1a黑线所围区域),均匀弥散分布于再结晶基体,其体积分数约为30%。大部分纳米孪晶界平直完整,孪晶界和孪晶内部依然残留大量位错(图1c)。统计结果显示,孪晶片层平

均厚度为28 nm,与退火前相当。选区电子衍射花样(图1b和c中插图)表明纳米孪晶/再结晶混合结构304样品仍为奥氏体结构。

塑性应变幅控制的纳米孪晶强化304 SS样品的低周疲劳结果如图2a所示。显然,与粗晶样品相比,引入30%纳米孪晶结构明显提高了304 SS样品的循环应力幅( $\Delta\sigma/2$ ),同时仍保持很高的疲劳寿命。当塑性应变幅( $\Delta\varepsilon_{\text{pl}}/2$ )为0.10%时,纳米孪晶强化304 SS的疲劳寿命为17000 cyc,约为粗晶疲劳寿命(20000 cyc)的85%。此外,与粗晶304 SS类似,纳米孪晶强化304 SS在疲劳过程中也发生循环软化, $\Delta\varepsilon_{\text{pl}}/2 = 0.10\%$ 时其 $\Delta\sigma/2$ 从438 MPa下降至疲劳断裂时的347 MPa。

为了定量比较纳米孪晶强化304 SS样品在不同应变幅时的软化程度,定义软化比( $R$ )为<sup>[12]</sup>:

$$R = \frac{\Delta\sigma/2|_{\text{max}} - \Delta\sigma/2|_N}{\Delta\sigma/2|_{\text{max}}} \quad (1)$$

式中, $\Delta\sigma/2|_N$ 和 $\Delta\sigma/2|_{\text{max}}$ 分别表示为第 $N$ 周次时应力

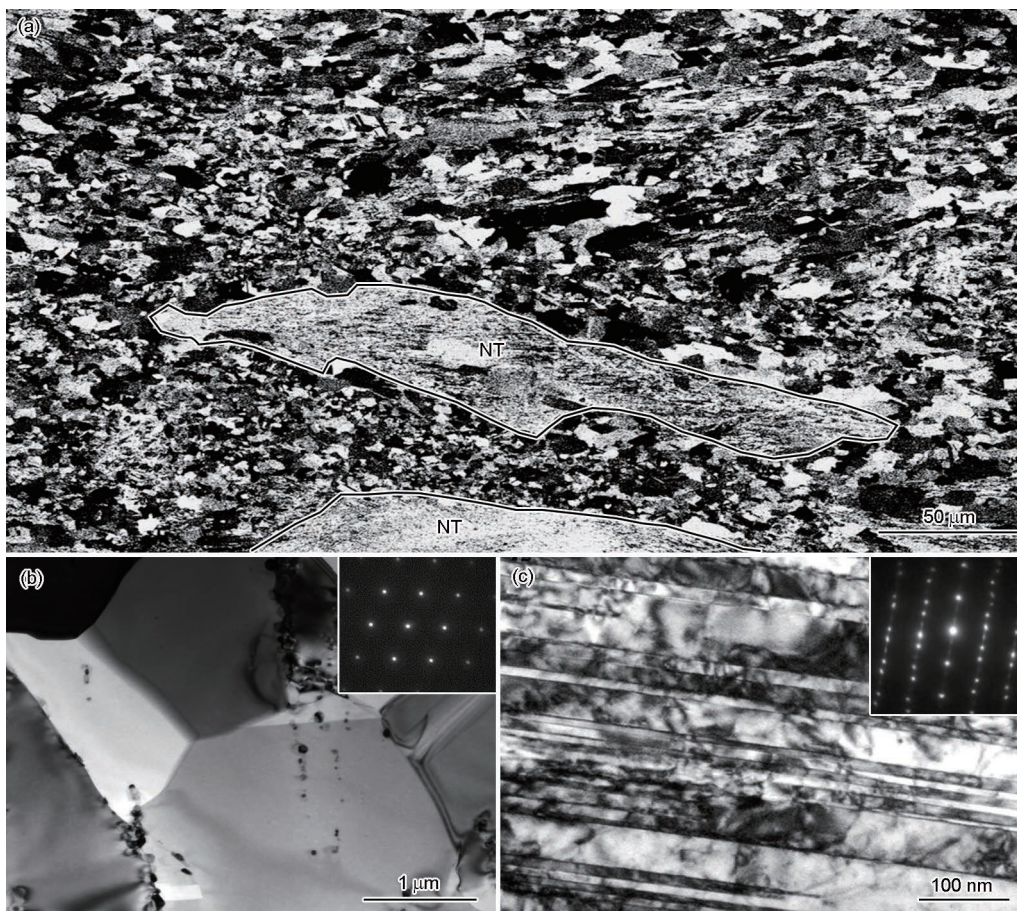


图1 纳米孪晶强化304不锈钢(304 SS)的微观结构

**Fig.1** Cross-sectional SEM image of nanotwin (NT)-strengthened 304 stainless steel (304 SS) comprising NT bundles embedded in micrometer-sized grain matrix (a), TEM images of static recrystallized (SRX) grains with few dislocations (b) and nanotwins with numerous dislocations (c) (Insets in Figs.1b and c are the selected area electron diffraction (SAED) patterns)



幅和疲劳过程中最大应力幅。图2b所示为对应图2a的软化比-归一化循环周次( $N/N_f$ , 其中 $N_f$ 为疲劳断裂寿命)曲线。可见,纳米孪晶强化304 SS样品与粗晶304 SS在不同塑性应变幅时呈现类似的软化特征:塑性应变幅愈小, $R$ 愈大,即软化程度愈明显。例如,在较低塑性应变幅时(0.05%),纳米孪晶强化304 SS样品的 $R$ 大于粗晶304 SS,即软化程度愈明显。但随塑性应变幅增加,其软化程度要小于粗晶304 SS。显然,这与传统纳米材料低周疲劳时随应变幅增加软化程度增大(软化比 $> 50\%$ )和疲劳寿命显著降低的趋势截然不同<sup>[2,8,15,36]</sup>。

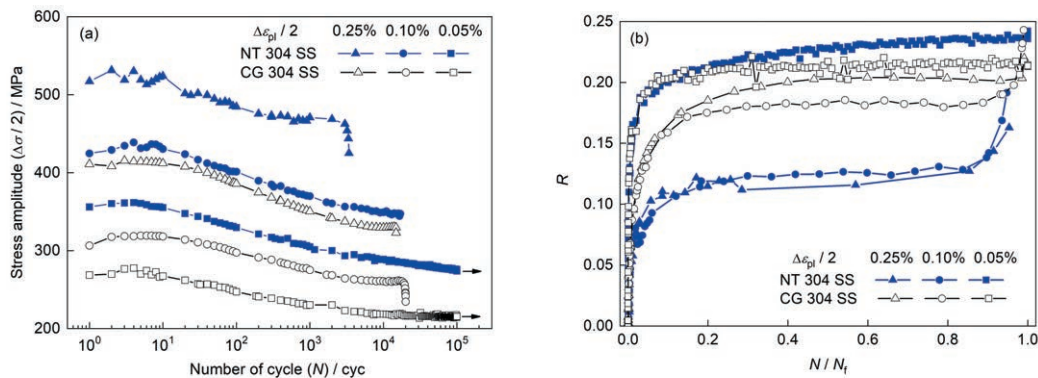


图2 纳米孪晶强化304 SS和粗晶304 SS的应变疲劳性能

Fig.2 Cyclic stress response curves (a) and corresponding cyclic softening ratio ( $R$ ) (b) of NT-strengthened 304 SS and coarse grained (CG) 304 SS under constant plastic strain amplitude ( $\Delta\epsilon_{pl}/2$ ) control (Arrows in Fig.2a denote the sample without failure,  $N_f$  denotes the fatigue-to-failure life)

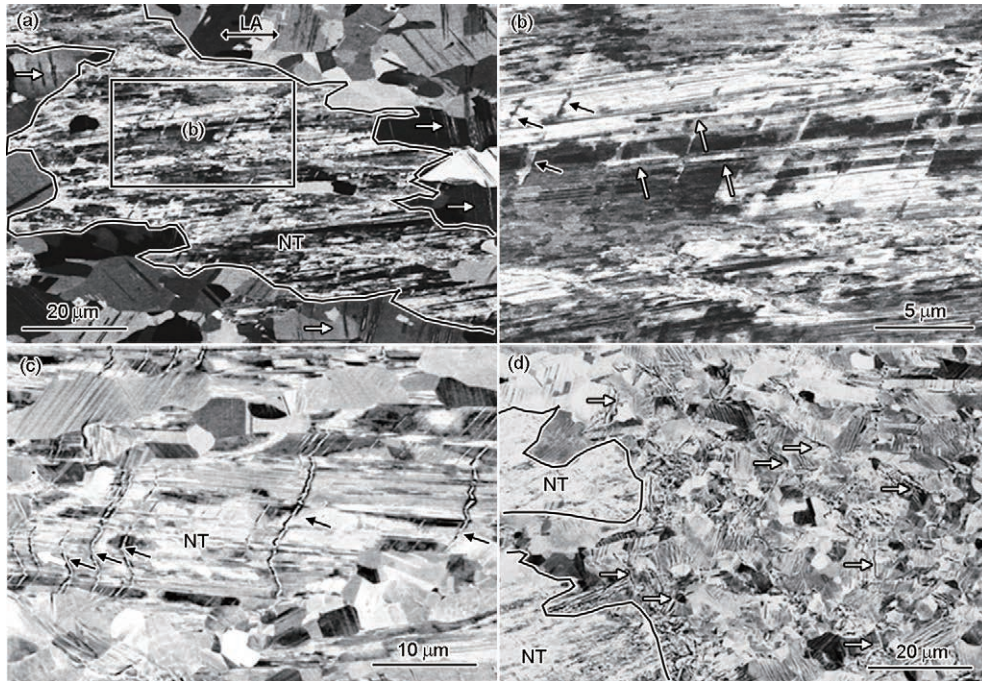


图3 纳米孪晶强化304 SS表面疲劳形貌特征

Fig.3 SEM image of surface fatigue features in NT strengthened 304 SS fatigued at  $\Delta\epsilon_{pl}/2$  of 0.05% (a, b) and 0.25% (c, d) (LA denotes the cyclic loading axis. The white arrows in Figs.3a and d denote the slip bands and crack in coarse grains, respectively. The black arrows in Figs.3b and c denote the zigzag slip bands across twin boundaries while the white ones in Fig.3b indicate the slip bands parallel to twin boundaries)

为了理解纳米孪晶混合结构的低周疲劳行为,首先表征了纳米孪晶强化304 SS样品在不同应变幅疲劳后的表面疲劳形貌(图3)。较低塑性应变幅(0.05%)疲劳时,在大部分纳米孪晶和再结晶晶粒表面并未发现明显的疲劳形貌特征,表明此条件下主要发生弹性变形。但部分纳米孪晶晶粒表面存在一些跨过许多孪晶片层的滑移带(如图3b中黑色箭头所示)和少量平行于孪晶界面的滑移带形貌(如图3b中白色箭头所示)。同时也观察到纳米孪晶周围很多再结晶晶粒出现滑移带形貌(如图3a中白色箭头所示),而在远离孪晶晶粒的再结晶表面却很少观察

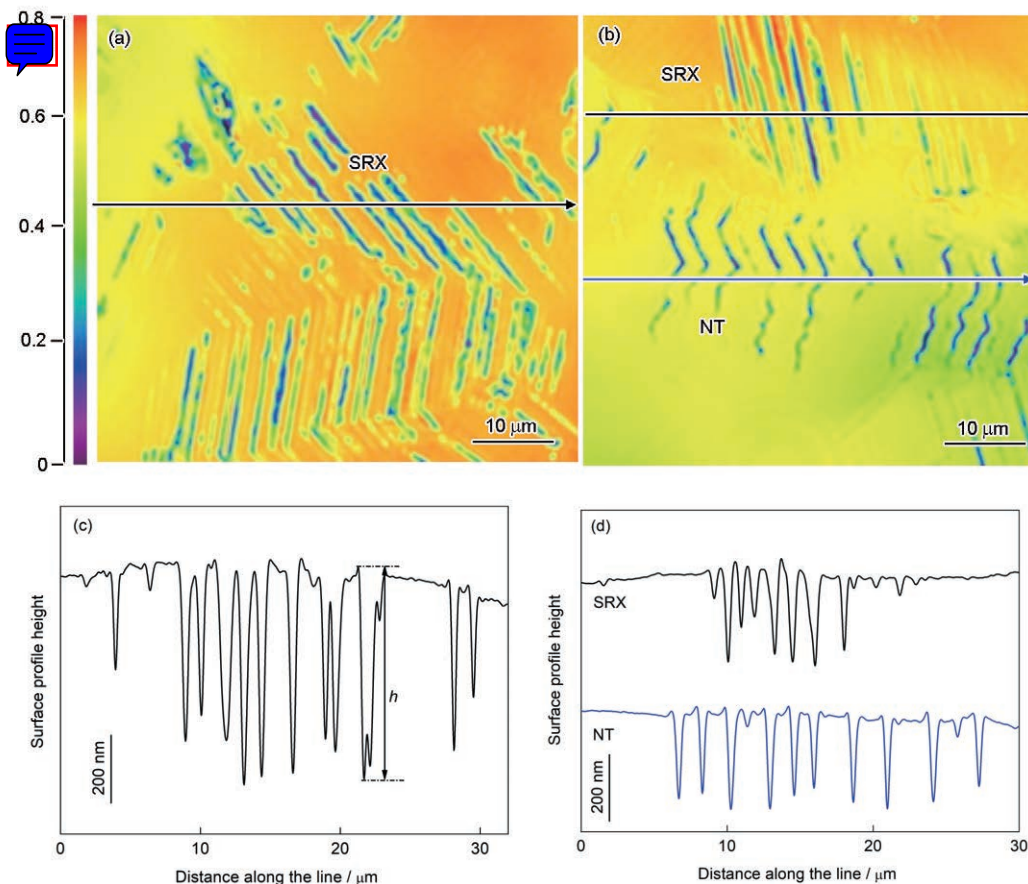
到明显变形特征。利用激光共聚焦显微镜表征发现纳米孪晶表面的滑移带平均起伏高度约为 $0.15\ \mu\text{m}$ ,远小于再结晶表面的滑移带高度(约 $0.61\ \mu\text{m}$ ,图4a和b),这与纳米孪晶强化304 SS应力控制高周疲劳特征类似<sup>[34]</sup>。

当塑性应变幅增至 $0.25\%$ ,在更多纳米孪晶晶粒及其周围再结晶晶粒表面发现明显滑移带,如图3c中黑色箭头所示。纳米孪晶晶粒表面跨过许多孪晶界的“Z”字型滑移带数目也明显增加,并且与周围再结晶晶粒中的滑移带在空间上几乎相连,也具有相同三维起伏高度( $0.47\sim 0.48\ \mu\text{m}$ ),如图4c和d所示。但是,在纳米孪晶晶粒表面,未发现低应变幅疲劳时平行孪晶界的滑移带形貌。此外,微米尺度的疲劳裂纹出现在具有明显滑移带特征的再结晶区域内(如图3d中白色箭头所示),但在再结晶晶粒与纳米孪晶界面附近未观察到。

纳米孪晶强化304 SS在不同应变幅疲劳后微观结构的TEM像见图5a、c和图6a、d。从图5a可见,在较低塑性应变幅(如 $0.05\%$ )疲劳时,大部分纳

米孪晶和再结晶晶粒的微观结构特征与疲劳前(图1b和c)类似:纳米孪晶界面具有优异的结构稳定性,保持平直、完整,仍存在高密度位错,与传统纳米金属疲劳时异常晶粒粗化不同<sup>[2,12,15]</sup>。仅在极少量纳米孪晶区域出现退孪生结构(如图5b黑色线所围区域):孪晶界上存在大量孪生台阶,孪晶片层平均间距增至 $138\ \text{nm}$ ,孪晶内出现高密度的位错特征(图5c)。此外,在纳米孪晶周围再结晶区域内,可见高密度平面位错列和部分细小的块状 $\alpha'$ 马氏体相(图5b黑色箭头所示),与应变控制高周疲劳特征类似<sup>[34]</sup>。这表明低塑性应变幅疲劳时纳米孪晶结构可与周围再结晶晶粒协同发生循环塑性变形。

在较高塑性应变幅( $0.25\%$ )时,大部分纳米孪晶结构表现出优异的疲劳稳定性(图6a),平均片层厚度为 $30\ \text{nm}$ (图6e),与初始态相当<sup>[34]</sup>。相对于低塑性应变幅疲劳特征(图5),此时更多纳米孪晶及其周围再结晶晶粒均协同承担循环塑性变形。高倍TEM观察发现,纳米孪晶内部出现了许多跨过孪晶界的项链位错形貌(如图6b中白色箭头所示)。其周围大



Color online

图4 纳米孪晶强化304 SS表面三维疲劳形貌特征

**Fig.4** CLSM images of 3-dimensional surface fatigue features in NT-strengthened 304 SS fatigued at  $\Delta\epsilon_{pl}/2$  of  $0.05\%$  (a) and  $0.25\%$  (b), and corresponding height fluctuation of slip band along the lines in Fig.4a ( $h$ —net height variation between adjacent hill and valley) (c) and Fig.4b (d)



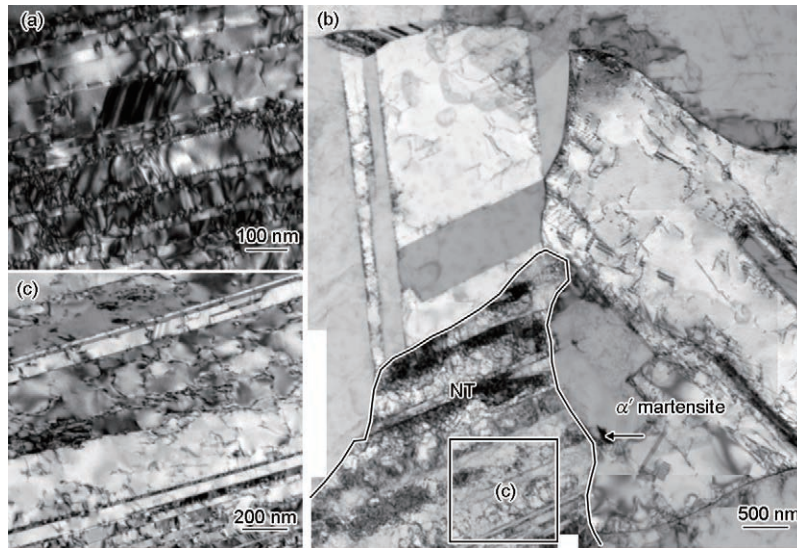


图5 纳米孪晶强化 304 SS 在低塑性应变幅(0.05%)疲劳时的微观结构特征

Fig.5 Bright-field TEM images of typical NT grain with intact twins (a) and detwinned structures in the vicinity of SRX grains in NT strengthened 304 SS fatigued at  $\Delta\epsilon_{pl} / 2$  of 0.05% (b), and TEM image of rectangle area in Fig.5b showing twin boundaries with steps and dislocation tangles in the twin interior (c)

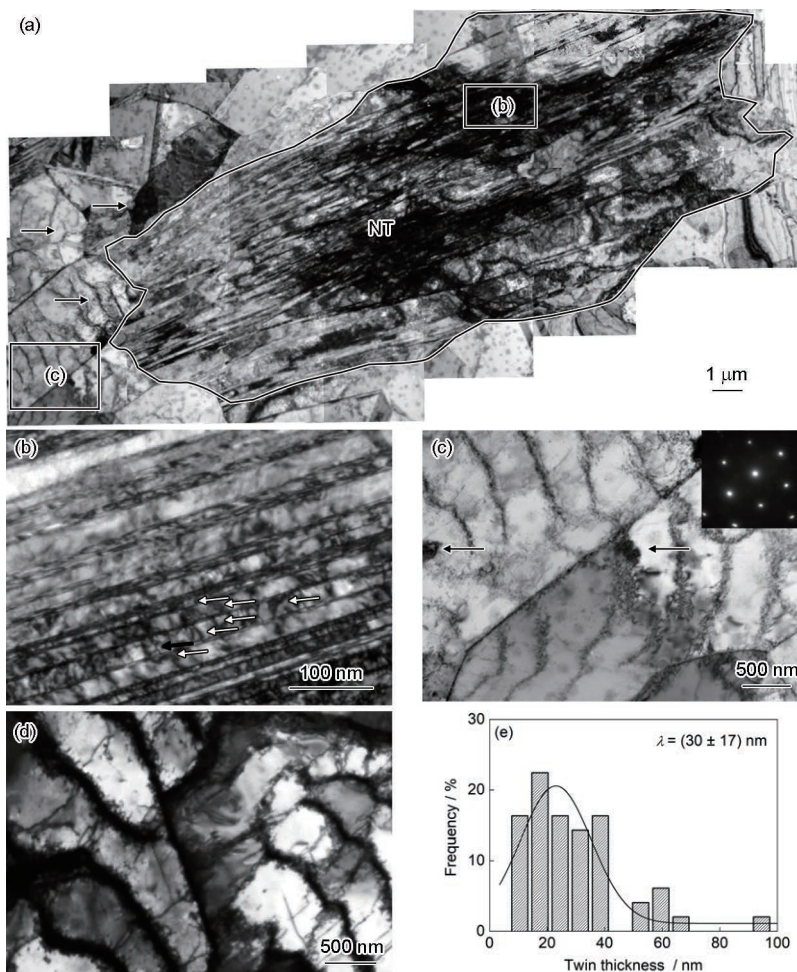


图6 纳米孪晶强化 304 SS 在高应变幅疲劳(0.25%)时的微观结构特征和孪晶片层厚度

Fig.6 Overview TEM images of the microstructure in NT-strengthened 304 SS fatigued at  $\Delta\epsilon_{pl} / 2$  of 0.25% (a), high-magnification image of one typical NT grain undergoing cyclic plastic strain with correlated necklace dislocations denoted by white arrows (b) and its surrounding SRX grains with tiny  $\alpha'$  martensite (denoted by the black arrows) around dislocation walls (c), compared to that far away from NT grains (d), and corresponding distribution of twin lamella thickness ( $\lambda$ ) (e) (The black arrows in Figs.6a denote dislocation cell in SRX, inset in Fig.6c is the SAED pattern)

部分再结晶区域内分布着高密度的规则位错组态,如位错胞和位错墙(图 6c);而部分位错胞附近也存在亚微米尺度的块状  $\alpha'$  马氏体相(如图 6c 中黑色箭头所示)。但在远离纳米孪晶结构的再结晶位内部,仅形成亚微米尺度的位错胞结构(图 6d)。

### 3 分析讨论

众所周知,材料的循环响应行为(循环流变应力水平、软化/硬化)和疲劳寿命主要与其微观结构以及疲劳变形机制密切相关<sup>[1,37,38]</sup>。粗晶 304 奥氏体不锈钢在常规塑性应变幅范围(即小于 0.25%)内疲劳时表现为循环软化,且在低应变幅时软化程度愈大(图 2)。这主要归因于低层错能金属疲劳时局部软取向晶粒内位错平面滑移模式导致较弱的位错间交互作用以及位错组态从高能态向低能态的演变<sup>[8,38-42]</sup>。

纳米孪晶强化 304 SS 不仅表现出高循环应力水平,亦保持与粗晶 304 SS 类似的循环软化程度和疲劳寿命,这首先与纳米孪晶结构及其循环变形机制相关。与传统纳米金属疲劳引起结构粗化行为不同,大部分纳米孪晶晶粒在不同塑性应变幅疲劳时均呈现出明显的结构稳定性(图 5 和 6)。究其原因,这里引入的孪晶界是一类特殊的共格晶界,其两侧的晶格呈镜面对称,因而界面能较低,仅为普通大角晶界的 1/10 左右,具有本征结构稳定性<sup>[3]</sup>。由于纳米孪晶强化 304 SS 样品中大部分纳米孪晶界与疲劳加载方向近似平行,纳米孪晶结构中可能出现一种独特的应变非局域化位错机制,即关联项链位错<sup>[26]</sup>,在孪晶通道内往复运动承担循环塑性应变,形成跨过许多孪晶界的“Z”字型滑移带形貌并且不破坏纳米孪晶结构的稳定性<sup>[26,28]</sup>。这与在应力控制高周疲劳过程中纳米孪晶的变形行为类似<sup>[34]</sup>。

相对于粗晶 304 SS,纳米孪晶强化 304 SS 的循环应力幅水平明显提高,这主要是由于稳定纳米尺度孪晶结构本身的高强度和高硬度(3.6 GPa)。纳米孪晶强化 304 SS 在低塑性应变幅疲劳时发生相对粗晶 304 SS 更明显的循环软化(图 2b)。这一方面与粗晶基体本身位错平面滑移模式和位错结构向低能量状态演变有关<sup>[8,38-42]</sup>;另一方面,部分纳米孪晶结构发生退孪生导致结构粗化和承载能力下降,也贡献循环软化。随塑性应变幅增加,纳米孪晶强化 304 SS 的循环软化程度减弱,也低于粗晶 304 SS。这与传统纳米结构材料“应变幅愈大,软化程度愈明显(软化比 > 50%)”的趋势截然不同。硬度测试结果表明,纳米孪晶结构在塑性应变幅 0.05% 和 0.25% 疲

劳后的平均硬度分别为 3.0 和 3.2 GPa,相对于初始态结构仅分别下降了 0.6 和 0.4 GPa。显然,纳米孪晶强化 304 SS 在应变控制疲劳时优异的抗循环软化能力主要得益于纳米孪晶结构本身优异的抗疲劳损伤变形能力和结构稳定性(图 5 和 6)。

除了本身参与塑性变形,纳米孪晶晶粒还协调相邻再晶晶粒发生显著的循环塑性变形,这主要归因于高强度纳米孪晶晶粒与再结晶基体较大的硬度或强度差异所引起的应变梯度和多轴应力状态<sup>[4,43]</sup>。在较低塑性应变幅疲劳时,相邻再晶晶粒主要以位错平面滑移为主。再结晶位与纳米孪晶相邻区域则发生一定程度的退孪生。在复杂应力条件下,具有较小滑移阻力的不全位错易激活,在长周次疲劳过程中引起显著退孪生,类似于磁控溅射纳米孪晶 Cu 样品疲劳引起的晶界附近严重退孪生区域<sup>[44,45]</sup>。退孪生机制本身一定程度上可协调循环塑性变形,并有利于缓解界面两侧的应变或应力集中。

随塑性应变幅增加,由于更大的弹塑性应变梯度和更高的应力水平<sup>[4,46]</sup>,纳米孪晶周围的再晶晶粒也发生更显著的塑性变形,导致高密度位错胞/墙结构和块状  $\alpha'$  马氏体的出现。纳米孪晶及其周围再晶晶粒通过位错运动、退孪生和马氏体相变等多种循环塑性变形机制的启动,有效协调了二者界面处的应变不相容性,显著抑制应变局域化,提高了抗疲劳损伤能力。因而,在纳米孪晶与周围再结晶界面附近很少出现疲劳裂纹,而大部分疲劳裂纹主要出现在发生严重塑性应变累积的再结晶区域。

纳米孪晶强化 304 奥氏体不锈钢具有较长的低周疲劳寿命主要归因于高强度纳米孪晶晶粒本身不仅可通过关联项链位错和退孪生机制承担塑性变形,亦可与周围再晶晶粒发生协同塑性变形,有效缓解了界面处的应力/应变集中,表现出良好的疲劳非局域化和抗裂纹萌生能力。高强度纳米孪晶结构不仅可以提高工程金属材料的强度和高周疲劳性能,亦可同时保持优异的低周疲劳性能,展示出更加广泛的潜在应用前景。

### 4 结论

(1) 结合大冲击能量动态塑性变形及后续退火处理工艺,成功制备了包含 30% (体积分数) 纳米孪晶结构的块体 304 奥氏体不锈钢样品。

(2) 塑性应变控制疲劳研究发现,引入纳米孪晶结构可明显提高 304 奥氏体不锈钢的循环应力水平,同时具有优异抗循环软化能力和疲劳寿命,与传



统纳米结构持续软化和较差疲劳寿命截然不同。这主要得益于纳米孪晶结构及其优异的循环稳定性和应变非局域化疲劳机理。

### 参考文献

- [1] Suresh S. Fatigue of Materials [M]. 2nd Ed., Cambridge, UK: Cambridge University Press, 1998: 679
- [2] Pineau A, Benzergha A A, Pardoën T. Failure of metals III: Fracture and fatigue of nanostructured metallic materials [J]. Acta Mater., 2016, 107: 508
- [3] Meyers M A, Chawla K K. Mechanical Behavior of Materials [M]. 2nd Ed., Cambridge, UK: Cambridge University Press, 2009: 739
- [4] Li Q, Yan F K, Tao N R, et al. Deformation compatibility between nanotwinned and recrystallized grains enhances resistance to interface cracking in cyclic loaded stainless steel [J]. Acta Mater., 2019, 165: 87
- [5] Majumdar S, Roy S, Ray K K. Fatigue performance of dual-phase steels for automotive wheel application [J]. Fatigue Fract. Eng. Mater. Struct., 2017, 40: 315
- [6] Wang Z G, Wang G N, Ke W, et al. Influence of the martensite content on the fatigue behavior of a dual-phase steel [J]. Mater. Sci. Eng., 1987, 91: 39
- [7] Anbarlooie B, Hosseini-Toudeshky H, Kadkhodapour J. High cycle fatigue micromechanical behavior of dual phase steel: Damage initiation, propagation and final failure [J]. Mech. Mater., 2017, 106: 8
- [8] Böhner A, Niendorf T, Amberger D, et al. Martensitic transformation in ultrafine-grained stainless steel AISI 304L under monotonic and cyclic loading [J]. Metals, 2012, 2: 56
- [9] Kaneko Y, Hayashi S, Vinogradov A. Cyclic response of SUS316L stainless steel processed by ECAP [J]. Mater. Trans., 2013, 54: 1612
- [10] Renk O, Hohenwarter A, Pippan R. Cyclic deformation behavior of a 316L austenitic stainless steel processed by high pressure torsion [J]. Adv. Eng. Mater., 2012, 14: 948
- [11] Ueno H, Kakihata K, Kaneko Y, et al. Enhanced fatigue properties of nanostructured austenitic SUS 316L stainless steel [J]. Acta Mater., 2011, 59: 7060
- [12] Höppel H W, Zhou Z M, Mughrabi H, et al. Microstructural study of the parameters governing coarsening and cyclic softening in fatigued ultrafine-grained copper [J]. Philos. Mag., 2002, 82A: 1781
- [13] Mughrabi H, Höppel H W, Kautz M. Fatigue and microstructure of ultrafine-grained metals produced by severe plastic deformation [J]. Scr. Mater., 2004, 51: 807
- [14] Kunz L, Lukáš P, Svoboda M. Fatigue strength, microstructural stability and strain localization in ultrafine-grained copper [J]. Mater. Sci. Eng., 2006, A424: 97
- [15] Mughrabi H, Höppel H W. Cyclic deformation and fatigue properties of very fine-grained metals and alloys [J]. Int. J. Fatigue, 2010, 32: 1413
- [16] Lu K. Stabilizing nanostructures in metals using grain and twin boundary architectures [J]. Nat. Rev. Mater., 2016, 1: 1
- [17] Lu K, Lu L, Suresh S. Strengthening materials by engineering coherent internal boundaries at the nanoscale [J]. Science, 2009, 324: 349
- [18] Sansoz F, Lu K, Zhu T, et al. Strengthening and plasticity in nanotwinned metals [J]. MRS Bull., 2016, 41: 292
- [19] Zhang X, Wang H, Chen X H, et al. High-strength sputter-deposited Cu foils with preferred orientation of nanoscale growth twins [J]. Appl. Phys. Lett., 2006, 88: 173116
- [20] Lu L, Chen X, Huang X, et al. Revealing the maximum strength in nanotwinned copper [J]. Science, 2009, 323: 607
- [21] Lu L, Shen Y F, Chen X H, et al. Ultrahigh strength and high electrical conductivity in copper [J]. Science, 2004, 304: 422
- [22] Lu L, You Z S. Plastic deformation mechanisms in nanotwinned metals [J]. Acta Metall. Sin., 2014, 50: 129  
(卢磊, 尤泽升. 纳米孪晶金属塑性变形机制 [J]. 金属学报, 2014, 50: 129)
- [23] Hodge A M, Furnish T A, Shute C J, et al. Twin stability in highly nanotwinned Cu under compression, torsion and tension [J]. Scr. Mater., 2012, 66: 872
- [24] Pan Q S, Lu L. Strain-controlled cyclic stability and properties of Cu with highly oriented nanoscale twins [J]. Acta Mater., 2014, 81: 248
- [25] Pan Q S, Lu Q H, Lu L. Fatigue behavior of columnar-grained Cu with preferentially oriented nanoscale twins [J]. Acta Mater., 2013, 61: 1383
- [26] Pan Q S, Zhou H F, Lu Q H, et al. History-independent cyclic response of nanotwinned metals [J]. Nature, 2017, 551: 214
- [27] Li X Y, Dao M, Eberl C, et al. Fracture, fatigue, and creep of nanotwinned metals [J]. MRS Bull., 2016, 41: 298
- [28] Lu L, Pan Q S, Hattar K, et al. Fatigue and fracture of nanostructured metals and alloys [J]. MRS Bull., 2021, 46: 258
- [29] You Z S, Li X Y, Gui L J, et al. Plastic anisotropy and associated deformation mechanisms in nanotwinned metals [J]. Acta Mater., 2013, 61: 217
- [30] Lu K, Yan F K, Wang H T, et al. Strengthening austenitic steels by using nanotwinned austenitic grains [J]. Scr. Mater., 2012, 66: 878
- [31] Yan F K, Liu G Z, Tao N R, et al. Strength and ductility of 316L austenitic stainless steel strengthened by nano-scale twin bundles [J]. Acta Mater., 2012, 60: 1059
- [32] Yi H Y, Yan F K, Tao N R, et al. Comparison of strength-ductility combinations between nanotwinned austenite and martensite-austenite stainless steels [J]. Mater. Sci. Eng., 2015, A647: 152
- [33] Yi H Y, Yan F K, Tao N R, et al. Work hardening behavior of nanotwinned austenitic grains in a metastable austenitic stainless steel [J]. Scr. Mater., 2016, 114: 133
- [34] Cui F, Pan Q S, Tao N R, et al. Enhanced high-cycle fatigue resistance of 304 austenitic stainless steel with nanotwinned grains [J]. Int. J. Fatigue, 2021, 143: 105994
- [35] Li Q, Yan F K, Tao N R. Enhanced fatigue damage resistance of nanotwinned austenitic grains in a nanotwinned stainless steel [J]. Scr. Mater., 2017, 136: 59
- [36] Meyers M A, Mishra A, Benson D J. Mechanical properties of nanocrystalline materials [J]. Prog. Mater. Sci., 2006, 51: 427
- [37] Mughrabi H. Fatigue, an everlasting materials problem-still en-



- vogue [J]. Proc. Eng., 2010, 2: 3
- [38] Peralta P, Laird C. Fatigue of metals [A]. Physical Metallurgy [M]. 5th Ed., Oxford: Elsevier, 2014: 1765
- [39] Bayerlein M, Christ H J, Mughrabi H. Plasticity-induced martensitic transformation during cyclic deformation of AISI 304L stainless steel [J]. Mater. Sci. Eng., 1989, A114: L11
- [40] Kelly P M. The martensite transformation in steels with low stacking fault energy [J]. Acta Metall., 1965, 13: 635
- [41] Krupp U, Roth I, Christ H J, et al. In situ SEM observation and analysis of martensitic transformation during short fatigue crack propagation in metastable austenitic steel [J]. Adv. Eng. Mater., 2010, 12: 255
- [42] Maier H J, Schneeweiss O, Donth B. Kinetics of fatigue-induced phase transformation in a metastable austenitic 304 L-type steel at low temperatures [J]. Scr. Metall. Mater., 1993, 29: 521
- [43] Yan F K, Tao N R, Archie F, et al. Deformation mechanisms in an austenitic single-phase duplex microstructured steel with nanotwinned grains [J]. Acta Mater., 2014, 81: 487
- [44] Shute C J, Myers B D, Xie S, et al. Microstructural stability during cyclic loading of multilayer copper/copper samples with nanoscale twinning [J]. Scr. Mater., 2009, 60: 1073
- [45] Shute C J, Myers B D, Xie S, et al. Detwinning, damage and crack initiation during cyclic loading of Cu samples containing aligned nanotwins [J]. Acta Mater., 2011, 59: 4569
- [46] Hong C S, Tao N R, Huang X, et al. Nucleation and thickening of shear bands in nano-scale twin/matrix lamellae of a Cu-Al alloy processed by dynamic plastic deformation [J]. Acta Mater., 2010, 58: 3103

(责任编辑:肖素红)